Real and effective thermal equilibrium in artificial square spin ices

Jason P. Morgan, Johanna Akerman, Aaron Stein, Charudatta Phatak, R. M. L. Evans, Sean Langridge, and Christopher H. Marrows

Phys. Rev. B **87**, 024405 — Published 9 January 2013

DOI: 10.1103/PhysRevB.87.024405

Real and effective thermal equilibrium in artificial square spin ice

Jason P. Morgan,[1] Johanna Akerman,[1,2] Aaron Stein,[3] Charudatta Phatak,[4]
R. M. L. Evans,[1] Sean Langridge,[5] and Christopher H. Marrows[1]

[1]*School of Physics and Astronomy,*
University of Leeds, Leeds LS2 9JT, United Kingdom
[2]*Instituto de Sistemas Optoelectrónicos y Microtecnología (ISOM),*
Universidad Politécnica de Madrid,
Avda. Complutense s/n, 28040 Madrid, Spain
[3]*Center for Functional Nanomaterials,*
Brookhaven National Laboratory, Upton, New York 11973, USA
[4]*Materials Science Division, Argonne National Laboratory,*
9700 South Cass Avenue, Argonne, Illinois 60439, USA
[5]*ISIS, STFC Rutherford Appleton Laboratory,*
Chilton, Didcot OX11 0QX, United Kingdom

Abstract

We have studied the magnetic microstates arising from single-shot thermalization processes that occur during growth in artificial square spin ices. The populations of different vertex types can be controlled by the system's lattice constant, as well as by depositing different material underlayers. The statistics of these populations are well-described by a simple model based on the canonical ensemble, which is used to infer an effective temperature for an arrested microstate. The normalized energy level spacings of the different magnetic vertex configurations are found to be very close to those predicted for a point dipole model: this is shown to be a very good approximation to energy level spacings calculated for finite-sized cuboid magnetic bodies. States prepared with a rotating field (an athermal method commonly used to lower the energy of these systems) cannot be described by this model, showing that such a method does not induce a near-equilibrium state.

PACS numbers: 75.50.Lk, 75.10.Hk, 75.25.-j, 75.75.-c

Theories of magnetism have long provided models for more complex statistical mechanical systems in physics and beyond. For instance, the venerable Ising model of a strongly anisotropic ferromagnet (famously exactly solved in two dimensional systems by Onsager,[1] and infamously unsolved in three dimensions) has been used in the context of describing the phase stability of ordered alloys,[2] the unbinding of DNA,[3] the structure of surfactant solutions,[4] and the behavior of neural networks.[5] Understanding systems that depart from equilibrium remains a challenge across all these fields.

The approach of constructing model magnetic systems that are comparatively easy to understand can be extended from theory to experiment in order to address this challenge. This is accomplished in the designer metamaterials known as artificial spin ices. They comprise an array of single-domain ferromagnetic islands, built using nanolithography,[6] that replicates much of the physics of pyrochlore crystal spin ice systems,[7] which in turn replicate the geometrical frustration of the proton disorder in water ice.[8] As all the parameters of the array may be engineered during fabrication, they allow for much wider exploration of phase space than the mere handful of naturally-occurring spin ices allow. Moreover, they are embodiments of statistical mechanical vertex models where the exact magnetic configuration (microstate) may be directly observed using advanced magnetic microscopy techniques.[9–11] Inspecting the microstate allows for such important statistical mechanical properties as the effective temperature of the system,[12,13] and its entropy,[14] to be directly determined from magnetic images, once the appropriate theoretical apparatus is in place.

The artificial square ice system we study here is depicted in Fig. 1(a). It is convenient to think of it as a lattice of vertices, at each of which four elements meet,[6,9,15] giving rise to six pairwise magnetostatic interactions of which at least two are frustrated. Hence, in the artificial square ice geometry there are four vertex types, according to the scheme defined in Ref. 6 by Wang *et al.*, which are depicted in Fig. 1(b). The magnetic moments at type 1 and type 2 vertices obey the two-in/two-out ice rule, satisfying four pairwise interactions, however, type 2 has a slightly higher energy as the two frustrated interactions are stronger. Both are magnetically charge neutral, although type 2 has a dipole moment. The twofold degenerate ground state consists of an antiferromagnetic tiling of the two type 1 vertices.[16] These two types contain all the vertices in the six-vertex model of square ice developed by Wu[17] and Lieb[18] to describe two-dimensional antiferroelectrics. The full sixteen vertex model has two more vertex types. Type 3 violates the ice rule, with a three-in(out)/one-

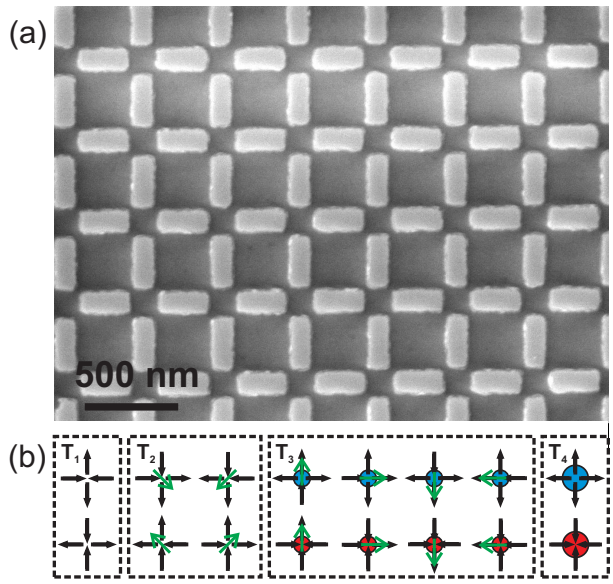

FIG. 1. (color online) Artificial square spin ice. (a) A scanning electron micrograph of one of our samples, showing the square lattice of vertices. (b) The various possible vertices, grouped into the four conventional types, denoted T_i for type i. Magnetic moments of the individual elements are represented by black arrows. T_1 and T_2 obey the ice rule. The magnetic charges of T_3 and T_4 are denoted by red and blue circles, and the net dipole moments of T_2 and T_3 by green arrows.

out(in) arrangement of the moments, hence it possesses both a magnetic charge and dipole moment, analogous to the monopole excitation of Castelnovo *et al.*[19] Type 4 has the highest energy, with all the moments pointing either in or out, and has a double magnetic charge but no dipole moment.

In their most common incarnations, artificial spin ices are athermal; the magnetostatic energy scales associated with the elements' local anisotropy and with their interactions exceed thermal energies by orders of magnitude at room temperature. (A recent exception has been reported by Kapaklis *et al.*[20], and some very preliminary data of thermally activated reversal are shown by Arnalds *et al.*[21]) Hence any dynamics in the system must be driven by the application of an external magnetic field. A number of reports have recently addressed dc-field magnetic reversal processes,[22–28] whilst low energy states are typically prepared using a rotating field ac demagnetization protocol,[6,10,23,29–31] which nevertheless does not lead to the ground state.[9] We have recently shown that thermally activated dynamics can take place during sample fabrication under the right conditions,[16] yielding a much closer approach to the ground state, although our sample too was in an arrested athermal state once fully

formed.

Our arrays were fabricated using electron beam lithography, evaporation of Permalloy, and lift-off.[16] Here we examined two sets of spin ice arrays. In the first set the magnetic elements were of size 270 nm $\times$ 115 nm $\times$ 25 nm, with variation between samples of the lateral dimensions of roughly $\pm$5 nm. The patterns were written together before being diced to allow the separate deposition of different underlayers (2 nm of Ti, 2 nm of Cr, or no underlayer, i.e. directly on the Si wafer surface). The deposition of the magnetic material for all these samples was then done simultaneously. The total size of each array was 0.5 mm $\times$ 0.5 mm, with lattice constants a ranging from 400–600 nm in order to vary the interaction strength.[6] Crucially, it has been shown that this deposition process leads to magnetic microstates that are thermalized,[16] which we have reproduced here in these new samples. As the elements grew, so did the energy scale of their magnetic shape anisotropies and interactions, eventually suppressing superparamagnetism and arresting their magnetic microstates. Each sample was subsequently imaged by magnetic force microscopy (MFM) over 13 μm $\times$ 13 μm areas in its as-grown state at five locations distributed across it. Error bars in any measured quantity hence arise as the standard error from averaging over these five images. The second set all had underlayers (2 nm of either Ta or Ti), and were slightly smaller (250 nm $\times$ 80 nm laterally), patterned over ~ 1 mm^2 total areas from multiple closely spaced 20 μm $\times$ 20 μm fields, but were otherwise very similar. These were ac demagnetized after growth, using rotating field protocols similar to those described in Ref. 29, and the microstates were also imaged by MFM at multiple locations.

In 2010, Nisoli *et al.* reported a formalism for inferring the effective temperature of such an athermal system from the vertex populations in its arrested microstate.[12] (The idea of effective temperatures in athermal systems is well known in the context of structural glasses[32,33] and granular media.[34]) The formalism defines vertices of type i to have fractional population n_i (with $\sum_i n_i = 1$), degeneracy q_i and energy E_i. It can be seen from Fig. 1b that $q_1 = 2$, $q_2 = 4$, $q_3 = 8$, and $q_4 = 2$. The vertex energy for each type E_i may then be calculated within a suitable magnetic model[35]. For the purposes of the calculations that follow, it is convenient to set the lowest energy $E_1 \equiv 0$ and measure the others relative to this, scaled such that $E_3 \equiv 1$.

Similarly to Ref. 12, we assume that the samples were close to thermal equilibrium up to the time at which they became arrested. These arrested states can then be described by a

canonical ensemble with a scaled temperature parameter β_{eff}, defining the effective temperature $T_{\text{eff}} = 1/k_{\text{B}}\beta_{\text{eff}}$, where k_{B} is Boltzmann's constant. For the field-demagnetized samples, the description is not so clear. Also following Ref. 12, we shall make a mean-field approximation, neglecting correlations between vertices. By Boltzmann's law, the probability of a given vertex being observed as type i is then given by

$$n_i = \frac{q_i \exp(-\beta_{\text{eff}} E_i)}{Z}, \tag{1}$$

where Z is the partition function and, to mean-field level, E_i is the energy of the four nanomagnets involved in a type-i vertex, in the presence of a surrounding medium of uncorrelated dipoles. A vertex randomly inserted into that state, and therefore uncorrelated with it, would have interactions with it that average to zero for all i, (the same will be true for an antiferromagnetically ordered state such as the ground state) so that only the six pairwise interactions of the vertex's four dipoles contribute to E_i,[11,15,36] which we have calculated using the same point-dipole approximation as in our previous work.[16] (Note, this yields different values of E_i from the four-charge Coulomb approximation used by Nisoli *et al.*[35]) For a typical microstate observed, the total energy calculated by a full sum over all pair-wise dipolar interactions differs by less than ~ 2 % from $\sum_i E_i n_i$, attributable to the fast decay of dipolar interactions with distance, and net long range interactions which largely cancel out due to a strongly demagnetized state (as well as possible statistical fluctuations due to the finite field-of-view of the MFM.) This same "counting vertices" calculation has previously been shown to work well for states consisting of excited vertex configurations on a ground state background.[16]

Eq. 1 leads straightforwardly to

$$\beta_{\text{eff}} E_i = \ln\left(\frac{q_i}{2}\frac{n_1}{n_i}\right). \tag{2}$$

Choosing $i = 3$, for instance, this allows β_{eff} to be determined from experimentally observed vertex populations in units of E_3^{-1}. In Fig. 2 we show two examples, prepared via the two routes, for which this formula yielded some of the lowest effective temperatures that we have observed. Fig. 2(a) shows an as-grown state that has thermally approached very closely to the ground state during deposition, before arrest — the image is featureless apart from a single domain wall that divides two incommensurate domains of ground-state order. We can use Eq. 2 to determine $\beta_{\text{eff}} E_3 = 7.4 \pm 0.5$, corresponding to a rather low T_{eff}. (Indeed

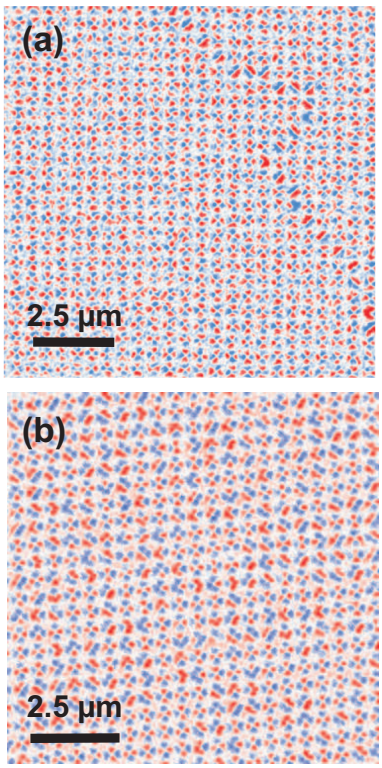

FIG. 2. (color online) MFM images of arrested magnetic microstates, with magnetic charge contrast shown using a red–white–blue color scheme. (a) An as-grown state in a sample of lattice constant 466 nm and no underlayer that closely approaches the ground state, with $\beta_{\rm eff} E_3 = 7.4 \pm 0.5$ based on the ratio n_1/n_3. (b) An icy state prepared by rotational ac demagnetization of a sample with lattice constant 500 nm, with $\beta_{\rm eff} E_3 = 2.18 \pm 0.05$ determined in the same way.

we have several images of this scale that show pure ground state order, yielding an effective temperature of zero, which is less useful for our later analysis since $\beta_{\rm eff}$ diverges.) Fig. 2(b) shows a state prepared using the rotating field protocol[29] ($\sim$ 10 Hz rotation frequency, initial field 1.3 kOe, field step size 10 Oe, field dwell time 7 s) where we find a much lower value $\beta_{\rm eff} E_3 = 2.20 \pm 0.04$. As expected, the sample that looks more magnetically disordered has the higher effective temperature.

In Fig. 3 we show our experimental data for a series of as-grown samples, with $\beta_{\rm eff} E_3$ determined using Eq. 2.[37] The differently shaped data markers indicate which underlayer (or lack thereof) the samples were grown on. All data acquired from the as-grown samples are well-described by the straightforward mean-field evaluation of the canonical ensemble expressed in Eq. 1, plotted as the solid lines in Fig. 3. We would like to emphasize that

these curves are not fitted to the data, they simply represent the predictions of the canonical ensemble with no free parameters.

We reach values of $\beta_{\text{eff}} E_3 \approx 7$ for the most strongly interacting arrays, much higher than the values achieved in Ref. 12 using the rotating field protocol, and also much higher than any we have achieved by that route. Empirically, we find that stronger interactions allow the system to more closely approach the ground state, and so the effective temperature is lower for more closely spaced arrays: within each series, increasing $\beta_{\text{eff}} E_3$ corresponds to smaller lattice constants,[37] as recently predicted in a comprehensive model of as-grown thermalization.[13]

By comparing the statistics for a given lattice constant,[37] we can see that this tendency to order is counteracted by the changes imparted by the different underlayers - $\beta_{\text{eff}} E_3$ is reduced with respect to the sample made directly on the Si surface. We infer that the additional surface roughness provided by the metal underlayers (which will be greater than that of the bare Si substrate) increases the level of quenched disorder in the system, broadening the distribution of magnetic island and vertex properties,[38–40] creating therefore an additional randomizing influence on the microstates formed. Within our model of the system as vertices of identical Ising point dipoles, increased interaction strength (quenched disorder) alters the equilibrium vertex distribution to yield a lower (higher) effective temperature by correlating (decorrelating) the system. Both are parameters by which the final statistical state of the system may be tuned,[6,41,42] consistent with Monte Carlo studies of thermally annealed square ice systems.[41]

This analysis is significantly simpler than the extended model presented by Nisoli *et al.* to describe their data from samples demagnetized with a rotating field.[12] The predictions of that model are shown as dotted lines in Fig. 3. Although it described the data from their rotating field samples extremely well for $\beta_{\text{eff}} E_3 < 3$, it performs poorly for our as-grown samples, especially for high values of β_{eff}, where it fails to predict an approach to the ground state. We would like to emphasize that both models make the same vertex gas approximation, so it is remarkable that our simplified model works so well at high β_{eff}, where correlations are expected to be important. A feature common to both protocols is the randomizing influence of quenched disorder which may be responsible for the acquisition of "thermal-like" vertex distributions following ac demagnetization, and at least appears to be a larger hinderance to GS formation during both thermal and field "annealing" of artificial

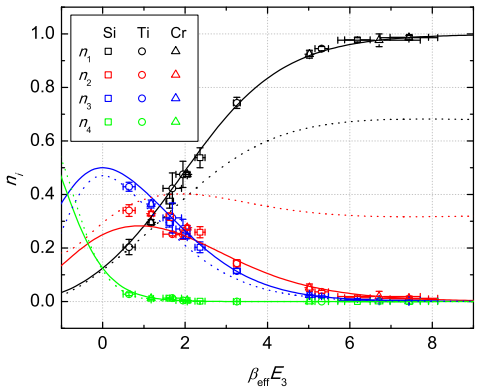

FIG. 3. (color online) Variation of vertex populations n_i with $\beta_{\rm eff}$. Experimental data points for as-grown samples on different substrates are shown with differently shaped data markers. The solid lines are the expected populations based on the simple canonical ensemble model with point dipole energies, whilst the dotted lines are the predictions of the extended model given in Ref. 12 that uses four-charge energies. The predictions of the models are very different for low effective temperatures (high $\beta_{\rm eff}E_3$), with the extended model not approaching the ground state as the data do.

square Ising lattices than the systems' frustrated geometries.[38,42,43]

The calculations in Ref. 12 differ from our simpler model based on the canonical ensemble in two ways. First, in order to modify the populations of the various vertex types, that extended model invented a distinction between the type 2 vertices that belonged to the uniform background provided by the high starting field and those that arise during demagnetization. It is this modification that prevents the dashed lines in Fig. 3 from approaching the ground state ($n_1 \to 1$) as $\beta_{\rm eff}$ becomes large. Instead, the extended model predicts a residue of type 2 vertices which tends to exactly one-third as $\beta_{\rm eff}$ increases, which our samples do not display. As the concept of initial (background) and final (defect) states has no meaning in thermal equilibrium we do not require this background of additional type 2 vertices.

Second, the vertex energies were calculated by Nisoli *et al.* by summing the Coulomb interactions of the four charges at the vertex, giving the ratio $E_2/E_3 = 0.453$,[12] whereas in our point dipole calculation, $E_2/E_3 = 0.692$. Here, we used our previously described point dipole model,[16] which we found was required to obtain a good match between our experimental data and the model used to describe them that is evident in Fig. 3. Aside

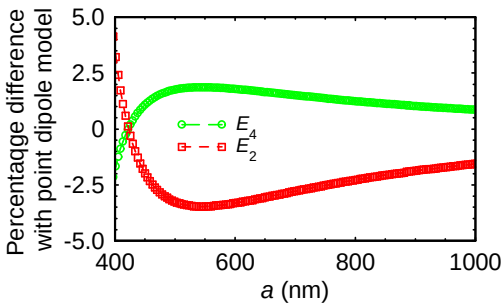

FIG. 4. (color online) The percentage departures of the energies E_i given by a calculation based on finite-sized magnetic bodies from the point dipole model, which are remarkably small even at small lattice constant a. E_1 and E_3 are not shown as they are defined to be 0 and 1.

from the fact that the data in Fig. 3 are well described by it, the use of this model, which might naïvely be expected to perform poorly for dense (strongly interacting) lattices, can be further justified.

We have used the model of Phatak *et al.*[44] to calculate exact values for the vertex energies in square ice for rectangular prism-shaped islands of our dimensions using the general framework proposed by De Graef and Beleggia for calculating the interactions of finite magnetic bodies.[45] The results of these calculations show that whilst the absolute energies for realistically shaped islands diverge from the point dipole approximation as a decreases, by as much as approximately a factor of two for shortest a, the ratios of these energies—on which our calculations here depend—are very closely reproduced by this model: to within better than 5 per cent, as shown in Fig. 4.[46] Whilst a marginally more accurate description of the system is possible using these exact energy calculations, the convenience of using the point dipole values for E_i is that they are a-invariant. Thus, all our data can be represented with a single model, at little expense to the energy approximation.

On the basis of Eq. 2, this energy ratio can be determined experimentally from the observed vertex populations as the ratio of $\ln(4n_1/2n_2)$ to $\ln(8n_1/2n_3)$. Figure 5 shows the relevant population data for all our as-grown samples, which again show good agreement with the prediction of the point dipole model (which is shown as a solid line), further justifying this choice. The slope returned by a proportional fit is 0.64 ± 0.02, suggesting that in reality there are some small departures from the energy levels predicted by this model. This difference can be accounted for partly by noting that the exact finite-body

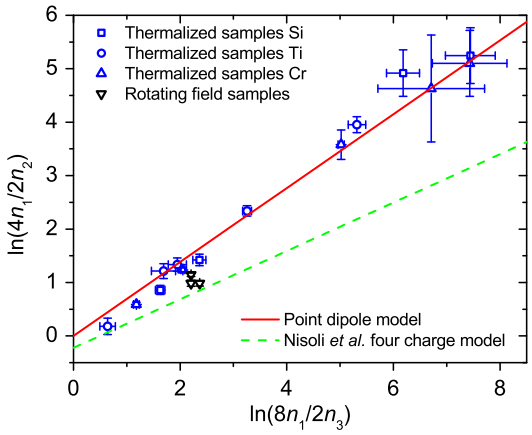

FIG. 5. (color online) The ratio of vertex energies E_2/E_3 can be determined experimentally as the slope of this plot. The data for our as-grown thermalized samples (circles) are well-described by the the point dipole model (solid line). The data from some rotating field demagnetized samples (triangles), which cluster at $\beta_{\rm eff}E_3 \approx 2.2$, sit between the predictions of the point dipole and four-charge approximation of Nisoli *et al.* (dashed line). Note that this line has an intercept of $\ln(4n_1/2n_2) = \ln(4/5)$, rather than passing through the origin, for consistency with the way that the model of Ref. 12 treats background vertices.

energy for E_2 is slightly less than that predicted by the point dipole model for most values of a (as seen in Fig. 4). The discrepancy can also be partly explained by considering that the magnetization of the real islands will depart slightly from the perfectly uniform state assumed in the calculations of Ref. 44, as has been shown to be the case by Lorentz microscopy studies,[27] which slightly relaxes the energy of type 2 vertex configurations.

It is striking that when the equivalent plot[47] was made in Ref. 12 for rotating field samples, a slope of 0.441 was obtained, implying that the four-charge model (not consistent with the mean field approach) better represents the energetics under those circumstances. We reproduce that calculation as a dashed line in Fig. 5, which clearly does not describe our data. It is interesting to consider the statistics of our field-demagnetized samples in this light: we plot the (rather closely clustered) points for three such samples as triangles in Fig. 5. Whilst they are too few to be conclusive, the data points lie between the predictions of the point dipole model and four-charge model. A fitted line (in this case using an intercept of $\ln(4/5)$ due to the additional degeneracy of the background vertex type) returns a gradient of $E_2/E_3 = 0.58 \pm 0.03$.

To conclude, we have confirmed that our close-to-ground state samples[16] have truly captured a thermally equilibrated state that can be described simply within the canonical ensemble, and that the degree of magnetic disorder, as captured by the effective temperature, may be controlled during the growth process, allowing for acquisition of strong GS order over a large parameter range. We have obtained states with effective temperatures that span a wide range, reaching a factor of two lower than those obtained using the athermal rotating field protocol.[12] Moreover, such athermally-prepared states require a theoretical description that requires the simple canonical ensemble picture to be modified quite drastically. They do not therefore correspond to an arrested snapshot of any thermally equilibrated state, as might be expected since the rotating field samples only ever make downward transitions in the energy landscape during the preparation of their microstate. These statistical differences in vertex-type population are experimentally detectable within the scheme of interpretation that we discuss here: a sample thermalized at a real temperature T and then arrested will not have the same statistics as a sample athermally prepared to have an effective temperature $T_{\rm eff}$.[48] In both cases, the effective temperature may be an instructive means of parameterizing the ratio between the contrary effects of interaction strength and quenched disorder in such systems. Pushing the limits of the nanofabrication of such magnetic arrays to give small enough element volumes to allow the onset of thermal fluctuations will permit us to explore the crossover between these regimes in a model system where the Hamiltonian is specified by design.

Note added in Proof: Since submitting the final version of our manuscript, we have become aware of related work on thermal routes to the ground state of square ice systems,[49] where the island thickness dependence of the vertex populations, shown in the inset of Fig. 5 of that report, is in good accord with the data we show here in Fig. 3.

ACKNOWLEDGMENTS

We would like to thank M. De Graef for sharing his code with us for computing the energy of the realistically shaped magnetic blocks. This work was supported by the (UK) EPSRC and the STFC Centre for Materials Physics and Chemistry. The research was carried out in part at the Center for Functional Nanomaterials, Brookhaven National Laboratory, which is supported by the US Department of Energy, Office of Basic Energy Sciences, under Contract

No. DE-AC02-98CH10886, and in part at Argonne National Laboratory, a US DOE Science Laboratory operated under contract number DE-AC02-06CH11357.

---

[1] L. Onsager, Phys. Rev. **65**, 117 (1944).

[2] A. Gonis, P. P. Singh, P. E. A. Turchi, and X.-G. Zhang, Phys. Rev. B **51**, 2122 (1995).

[3] R. Bundschuh and U. Gerland, Eur. Phys. J. E **19**, 319 (2006).

[4] D. Roux, C. Coulon, and M. E. Cates, J. Chem. Phys. **96**, 4174 (1992).

[5] J. J. Hopfield, Proc. Natl. Acad. Sci. USA **79**, 2554 (1982).

[6] R. F. Wang, C. Nisoli, R. S. Freitas, J. Li, W. McConville, B. J. Cooley, M. S. Lund, N. Samarth, C. Leighton, V. H. Crespi, and P. Schiffer, Nature (London) **439**, 303 (2006).

[7] S. T. Bramwell and M. J. P. Gingras, Science **294**, 1495 (2001).

[8] L. Pauling, J. Am. Chem. Soc. **57**, 2680 (1935).

[9] C. Nisoli, R. Wang, J. Li, W. F. McConville, P. E. Lammert, P. Schiffer, and V. H. Crespi, Phys. Rev. Lett. **98**, 217203 (2007).

[10] Y. Qi, T. Brintlinger, and J. Cumings, Phys. Rev. B **77**, 094418 (2008).

[11] E. Mengotti, L. Heyderman, A. Rodríguez, A. Bisig, L. Le Guyader, F. Nolting, and H. Braun, Phys. Rev. B **78**, 144402 (2008).

[12] C. Nisoli, J. Li, X. Ke, D. Garand, P. Schiffer, and V. H. Crespi, Phys. Rev. Lett. **105**, 047205 (2010).

[13] C. Nisoli, New J. Phys. **14**, 035017 (2012).

[14] P. E. Lammert, X. Ke, J. Li, C. Nisoli, D. M. Garand, V. H. Crespi, and P. Schiffer, Nature Phys. **6**, 786 (2010).

[15] G. Möller and R. Moessner, Phys. Rev. Lett. **96**, 237202 (2006).

[16] J. P. Morgan, A. Stein, S. Langridge, and C. H. Marrows, Nature Phys. **7**, 75 (2011).

[17] F. Y. Wu, Phys. Rev. Lett. **18**, 605 (1967).

[18] E. H. Lieb, Phys. Rev. Lett. **18**, 1046 (1967).

[19] C. Castelnovo, R. Moessner, and S. L. Sondhi, Nature (London) **451**, 42 (2008).

[20] V. Kapaklis, U. B. Arnalds, A. Harman-Clarke, E. Th. Papaioannou, M. Karimipour, P. Korelis, A. Taroni, P. C. W. Holdsworth, S. T. Bramwell, and B. Hjörvarsson, New J. Phys. **14**, 035009 (2012).

[21] U. B. Arnalds, A. Farhan, R. V. Chopdekar, V. Kapaklis, A. Balan, E. Th. Papaioannou, M. Ahlberg, F. Nolting, L. J. Heyderman, and B. Hjörvarsson, Appl. Phys. Lett. **101**, 112404 (2012).

[22] S. Ladak, D. E. Read, G. K. Perkins, L. F. Cohen, and W. R. Branford, Nature Phys. **6**, 359 (2010).

[23] A. Schumann, B. Sothmann, P. Szary, and H. Zabel, Appl. Phys. Lett. **97**, 022509 (2010).

[24] E. Mengotti, L. J. Heyderman, A. Fraile Rodríguez, F. Nolting, R. V. Hügli, and H. B. Braun, Nature Phys. **7**, 68 (2011).

[25] S. Ladak, D. Read, T. Tyliszczak, W. R. Branford, and L. F. Cohen, New J. Phys. **12**, 023023 (2011).

[26] J. P. Morgan, A. Stein, S. Langridge, and C. H. Marrows, New J. Phys. **13**, 105002 (2011).

[27] C. Phatak, A. K. Petford-Long, O. Heinonen, M. Tanase, and M. De Graef, Phys. Rev. B **83**, 174431 (2011).

[28] S. D. Pollard, V. Volkov, and Y. Zhu, Phys. Rev. B **85**, 180402 (2012).

[29] R. F. Wang, C. Nisoli, R. S. Freitas, J. Li, W. McConville, B. J. Cooley, M. S. Lund, N. Samarth, C. Leighton, V. H. Crespi, and P. Schiffer, J. Appl. Phys. **101**, 09J104 (2007).

[30] X. Ke, J. Li, C. Nisoli, P. E. Lammert, W. McConville, R. F. Wang, V. H. Crespi, and P. Schiffer, Phys. Rev. Lett. **101**, 037205 (2008).

[31] N. Rougemaille, F. Montaigne, B. Canals, A. Duluard, D. Lacour, M. Hehn, R. Belkhou, O. Fruchart, S. El Moussaoui, A. Bendounan, and F. Maccherozzi, Phys. Rev. Lett. **106**, 057209 (2011).

[32] R. Di Leonardo, L. Angelani, G. Parisi, and G. Ruocco, Phys. Rev. Lett. **84**, 6054 (2000).

[33] N. Greinert, T. Wood, and P. Bartlett, Phys. Rev. Lett. **97**, 265702 (2006).

[34] A. Mehta and S. F. Edwards, Physica A **157**, 1091 (1989).

[35] Nisoli *et al.*[12] added up the Coulomb interactions between the four poles found at the center of a vertex, which produces values roughly in accordance with micromagnetic calculations[50] for a single isolated vertex.

[36] L. A. Mól, R. L. Silva, R. C. Silva, A. R. Pereira, W. A. Moura-Melo, and B. V. Costa, J. Appl. Phys. **106**, 063913 (2009).

[37] See Supplemental Material at [URL will be inserted by publisher] for full details of all the populations n_i in our various as-grown thermalized samples, as well as the values of βE_2 and

βE_3 derived from them.

[38] A. Libál, C. J. Olson Reichhardt, and C. Reichhardt, Phys. Rev. Lett. **102**, 237004 (2009).

[39] S. Daunheimer, O. Petrova, O. Tchernyshyov, and J. Cumings, Phys. Rev. Lett. **107**, 167201 (2011).

[40] Z. Budrikis, P. Politi, and R. L. Stamps, J. Appl. Phys. (2012).

[41] Z. Budrikis, K. L. Livesey, J. P. Morgan, J. Akerman, A. Stein, S. Langridge, C. H. Marrows, and R. L. Stamps, New J. Phys. **14**, 035014 (2012).

[42] Z. Budrikis, J. P. Morgan, J. Akerman, A. Stein, R. L. Stamps, P. Politi, S. Langridge, and C. H. Marrows, Phys. Rev. Lett. **109**, 037203 (2012).

[43] D. Davidović, S. Kumar, D. Reich, J. Siegel, S. Field, R. C. Tiberio, R. Hey, and K. Ploog, Phys. Rev. Lett. **76**, 815 (1996).

[44] C. Phatak, M. Pan, A. K. Petford-Long, S. Hong, and M. De Graef, New. J. Phys. **14**, 075028 (2012).

[45] M. De Graef and M. Beleggia, J. Magn. Magn. Mater. **321**, L45 (2009).

[46] See Supplemental Material at [URL will be inserted by publisher] for a plot of the full normalised energies E_i calculated using the model of De Graef and Beleggia for realistically-shaped magnetic bodies[45].

[47] The equivalent graph made by Nisoli *et al.* in Ref. 12 plotted $\ln(5n_1/2n_2)$ on the ordinate, due to their use of an "anomalous" $q_2 = 5$ to represent the presence of the type 2 background at high effective temperatures, required to ensure that the data can be fitted by a line that passes through the origin.

[48] G. Bertotti, Phys. Rev. Lett. **76**, 1739 (1996).

[49] S. J. Greaves and H. Muraoka, J. Appl. Phys. **112**, 043909 (2012).

[50] R. Wang, *Geometrical magnetic frustration and demagnetization of artificial spin ice*, Ph.D. thesis, Pennsylvania State University (2007).